INTERNATIONAL JOURNAL FOR NUMERICAL METHODS IN ENGINEERING, VOL. 38, 2413–2431 (1995)

A CONSISTENT DXDR METHOD FOR ELASTIC–PLASTIC PROBLEMS

M. KADKHODAYAN AND L. C. ZHANG†

Department of Mechanical and Mechatronic Engineering, The University of Sydney, NSW 2006, Australia

SUMMARY

This paper proposed a new efficient method, the consistent DXDR method, for analysing general elastic-plastic problems. Two important factors in computational plasticity, the convergence and stability, were addressed. The method was constructed through a natural combination of two vital components: the DXDR algorithm which had been proved to be a powerful equation solver developed by the authors and a stable consistent algorithm for the integration of the constitutive equations of plasticity. Numerical examples demonstrated in detail the efficiency, accuracy, and stability attainable in solving various engineering problems.

KEY WORDS: consistent algorithm; plastic deformation; dynamic relaxation; computational stability; convergence rate

1. INTRODUCTION

In order to analyse various engineering problems with both material and geometrical non-linearity, a stable and efficient numerical method is essential. Consequently, the development of powerful algorithms suitable for a wide range of complex problems has been an important subject for many decades.

A newly developed dynamic relaxation method, the DXDR method,[1] has shown its promising potential with a number of distinguished features. For example, it is very reliable and stable for seeking an equilibrium state for non-linear problems; it has a fixed simple algorithm so that the programming becomes straightforward; and it needs not to solve large scale equations directly because of its explicit formulation. However, in the application of the DXDR method to elastic–plastic problems, a direct and important issue is how to combine an appropriate algorithm for integrating the constitutive equations over a discrete sequence of incremental steps. This algorithm should have a higher stability in dealing with the integration of the constitutive equations and in the mean time possess a higher compatibility with the DXDR method (an ability to enhance the merits of this method).

Recently, the conception of consistency between the tangent operator and the integration algorithm has received increasing attention and been found to play an important role in preserving the quadratic rate of asymptotic convergence of iteration solution.[2] It has been shown that if a consistency condition is satisfied, the stress increment predicted by the tangent operator based on the strain increment will correspond to the stress increment predicted by the integration procedure to the first order. In other words, the stability of the algorithm to integrate the constitutive equations would be guaranteed by using a tangent operator consistent with the

† Author to whom correspondence should be addressed

CCC 0029–5981/95/142413–19
© 1995 by John Wiley & Sons, Ltd.
Received 24 January 1994
Revised 12 September 1994

algorithm. This algorithm is much more stable than the continuum one, allows larger load steps and in turn reduces computational time and cost to a great extent. Furthermore, it provides high accuracy for both single step and subincrementation schemes and does not require the computation of contact stresses on the yield surface. Obviously, such a consistent algorithm is what the DXDR method would seek for.

It is therefore the purpose of this paper to investigate the generation of a new numerical method for general elastic–plastic problems by a natural combination of the DXDR method with the consistent algorithm. Emphasis is focused on the exploration of the accuracy, stability, efficiency and compatibility of the new method for solving various engineering problems.

2. PRINCIPLE OF THE DXDR METHOD

The DXDR method, like other modified dynamic relaxation approaches,[3,4] searches for the static solution of an equilibrium system by making use of the dynamic transient analysis and following a standard solution procedure. Therefore, the governing equations of a static system,

$$\mathbf{P}(\mathbf{X}) = \mathbf{F} \tag{1}$$

is replaced by its corresponding dynamic ones,

$$\mathbf{M}\ddot{\mathbf{X}} + \mathbf{C}\dot{\mathbf{X}} + \mathbf{P}(\mathbf{X}) = \mathbf{F} \tag{2}$$

where the mass and damping matrices, $\mathbf{M}$ and $\mathbf{C}$, are fictitiously chosen as diagonal ones so that the static solution could be obtained in a minimum number of pseudo-time steps. All the calculations become explicit when the central finite difference scheme is used. The explicit formulation for the solution vector $\mathbf{X}$ is given by

$$\dot{\mathbf{X}}_i^{n+1/2} = \frac{2 - \tau^n \zeta_i^n}{2 + \tau^n \zeta_i^n} \dot{\mathbf{X}}_i^{n-1/2} + \frac{2\tau^n}{2 + \tau^n \zeta_i^n} (\mathbf{m}_{ii}^n)^{-1} \mathbf{R}_i^n \tag{3a}$$

$$\mathbf{X}_i^{n+1} = \mathbf{X}_i^n + \tau^{n+1} \dot{\mathbf{X}}_i^{n+1/2}, \quad (i = 1, \ldots, N_{\text{total}}) \tag{3b}$$

where τ^n is the pseudo-time increment of the nth iteration and $\mathbf{R}^n = \mathbf{F} - \mathbf{P}(\mathbf{X}^n)$. In the derivation of equations (3), the following relations has been applied:

$$\begin{aligned} \mathbf{C}_{ii} &= \zeta_i \mathbf{m}_{ii} \quad (i = 1, \ldots, N_{\text{total}}) \\ \dot{\mathbf{X}}^{n-1/2} &= (\mathbf{X}^n - \mathbf{X}^{n-1})/\tau^n \\ \ddot{\mathbf{X}}^n &= (\dot{\mathbf{X}}^{n+1/2} - \dot{\mathbf{X}}^{n-1/2})/\tau^n \end{aligned} \tag{4}$$

where ζ_i^n is the node damping factor at the nth iteration and is calculated by

$$\zeta_i^n = 2\left(\frac{(\mathbf{X}_i^n)^{\mathrm{T}} \mathbf{p}_i^n}{(\mathbf{X}_i^n)^{\mathrm{T}} \mathbf{m}_{ii}^n \mathbf{X}_i^n}\right)^{1/2} \tag{5}$$

The initial $\tilde{\mathbf{X}}^0$ for iteration is determined by

$$\tilde{\mathbf{X}}^0 = \tfrac{1}{2}(\mathbf{X}^0 + \mathbf{X}^*) \tag{6}$$

where $\mathbf{X}^0$ and $\mathbf{X}^*$ indicate, respectively, the initially guessed solution and the peaks of locus of $\mathbf{X}$ during iteration without damping.[1] The elements of $\mathbf{M}$ are determined by the Gerschgörin theorem, i.e.

$$m_{ii}^L \geqslant \tfrac{1}{4}(\tau^n)^2 \sum_j |k_{ij}| \quad (L = u, v, w) \tag{7}$$

where m_{ii}^L is the fictitious mass in direction L on node i (whereas $\mathbf{m}_{ii}$ in the equation (5) is the fictitious submass matrix for each node), and k_{ij} is the element of the stiffness matrix $\mathbf{K}$ determined by

$$\mathbf{K} = \frac{\partial \mathbf{P}(\mathbf{X})}{\partial \mathbf{X}} \tag{8}$$

The complete algorithm of the DXDR method could then be written as:

(a) $\dot{\mathbf{X}}^0 = 0$, $n = 0$; specify $\mathbf{X}^0$, $N_{\max}$, e_R and e_k, where e_R and e_k are the convergence indexes of the residual force and energy, respectively,
(b) $\zeta_i^0 = 0$ $(i = 1, \ldots, N_{\text{total}})$; exert boundary conditions,
(c) determine $\tilde{\mathbf{X}}^0$ and iterate if necessary,
(d) form $\mathbf{M}$,
(e) calculate disequilibrium force $\mathbf{R}^n$,
(f) if $|R_i^{Ln}| \leqslant e_R (L = u, v, w)$, stop; otherwise continue,
(g) calculate ζ_i^n,
(h) obtain $\dot{\mathbf{X}}^{n+1/2}$,
(i) if $\sum_{L=u}^{w} \sum_{i=1}^{N} (\dot{x}_i^{Ln+1/2})^2 \leqslant e_k$, stop; otherwise continue,
(j) calculate $\mathbf{X}^{n+1}$,
(k) apply boundary conditions,
(l) $n = n + 1$; if $n > N_{\max}$, stop; otherwise return to step (d).

3. CONSISTENT INTEGRATION OF CONSTITUTIVE EQUATIONS

3.1. Integration algorithms of constitutive equations

Algorithms for the integration of constitutive equations play a central role in the analysis of elastic–plastic problems. The advantages and disadvantages of different methods, including the order of accuracy, stability, explicitness, and the rate of asymptotic convergence have been investigated extensively. Ortiz and Popov[5] generalized the *trapezoidal* and *midpoint rules* and investigated the numerical stability and accuracy. Nagtegaal and de Jong[6] proved the conditional stability of *tangent stiffness-radial corrector method.* R. D. Krieg and D. B. Krieg[7] studied the accuracy of this method for a non-hardening material and Schreyer *et al.*[8] investigated it for an isotropic hardening material with a constant plastic modulus. In parallel, Rice and Tracey[9] presented the *mean normal method* for the plane strain condition with non-hardening materials. Wilkins[10] and Mendelson[11] proposed the *elastic predictor-radial return method.* Argyris *et al.*[12] discussed the stability of integration procedures for inelasticity. Ortiz and Simo[13] studied the accuracy problem of the *return mapping algorithm* and Krieg and Key[14] extended the algorithm to involve isotropic and kinematic hardening properties.

Yoder and Whirley[15] demonstrated that there was an overall superiority of the *radial return method* over the other algorithms, particularly in the presence of hardening. Geometrically, this

method aims at finding the shortest distance of a point to a convex set. Within this framework, Simo and Taylor[2] suggested *consistent tangent operators* for rate-independent elastic–plastic problems. An extension of this algorithm under plane stress condition with mixed hardening has been provided by Dodds.[16]

The *generalized trapezoidal rule* (*GTR*) has the most distinguished characteristics in application. For instance, by using the flow rule associated with von Mises criterion and isotropic hardening, GTR gives

$$\boldsymbol{\sigma}_{n+1} = \boldsymbol{\sigma}_n + \mathbf{d}\boldsymbol{\sigma}_e - 2G\,\mathbf{de}^p$$

$$\mathbf{de}^p = \lambda[(1-\gamma)\mathbf{n}_n + \gamma\mathbf{n}_{n+1}] \tag{9}$$

$$\phi_{n+1}(\mathbf{s}_{n+1}, \bar{\sigma}_{n+1}) = 0$$

where G is the shear modulus, $\mathbf{s}$ is the deviatoric stress, and $\mathbf{d}\boldsymbol{\sigma}_e$ is the elastic stress increment corresponding to the strain increment. The incremental parameter λ is determined by the condition that the updated stresses satisfy the consistency equation, $\phi_{n+1} = 0$. The parameter γ may vary from 0 to 1, but if associated with the von Mises surface, the integration procedure becomes unconditionally stable when $\gamma \geqslant \frac{1}{2}$ and conditionally stable when $\gamma < \frac{1}{2}$.[7] $\mathbf{n}$ is a unit vector normal to the yield surface at the contact point and $\bar{\sigma}$ is the effective stress.

The relationship between different integration procedures could simply be classified as follows:

Integration procedures
- (1) *GTR*
  - (*a*) *Tangent predictor-radial return*[16] ($\gamma = 0$): *i.e. the commonly used continuum algorithm*
  - (*b*) *Mean normal*[16] ($\gamma = \frac{1}{2}$)
  - (*c*) *Elastic predictor-radial corrector*[2,16] ($\gamma = 1$)
- (2) *Mid-point rule* (*MR*): *it becomes the GTR when von Mises criterion and linear hardening are used*

3.2. *Continuum and consistent elastic–plastic tangent operators*

Based on the above-mentioned procedures, the continuum and consistent operators can be derived as follows

3.2.1. The continuum operator. The general relationship between the incremental stress and strain in the elastic–plastic regime may be written as

$$\mathbf{d}\boldsymbol{\sigma} = \mathbf{C}_{ep}\mathbf{d}\boldsymbol{\varepsilon} \tag{10}$$

where $\mathbf{C}_{ep}$ is the elastic–plastic stress strain matrix. If the operator $\mathbf{C}_{ep}$ is derived based on the method (1-a), the tangent predictor of the continuum moduli will be produced. For the flow rule

associated with von Mises criterion and isotropic hardening, the general form of this operator is

$$\mathbf{C}_{ep} = \frac{\mathbf{E}}{1+\nu}\begin{bmatrix} \frac{1-\nu}{1-2\nu}-\frac{s_x^2}{\Omega} & & & & & & \text{Sym.} \\ \frac{\nu}{1-2\nu}-\frac{s_x s_y}{\Omega} & \frac{1-\nu}{1-2\nu}-\frac{s_y^2}{\Omega} & & & & & \\ \frac{\nu}{1-2\nu}-\frac{s_x s_z}{\Omega} & \frac{\nu}{1-2\nu}-\frac{s_y s_z}{\Omega} & \frac{1-\nu}{1-2\nu}-\frac{s_z^2}{\Omega} & & & & \\ -\frac{s_x\tau_{xy}}{\Omega} & -\frac{s_y\tau_{xy}}{\Omega} & -\frac{s_z\tau_{xy}}{\Omega} & \frac{1}{2}-\frac{\tau_{xy}^2}{\Omega} & & & \\ -\frac{s_x\tau_{yz}}{\Omega} & -\frac{s_y\tau_{yz}}{\Omega} & -\frac{s_z\tau_{yz}}{\Omega} & -\frac{\tau_{xy}\tau_{yz}}{\Omega} & \frac{1}{2}-\frac{\tau_{yz}^2}{\Omega} & & \\ -\frac{s_x\tau_{zx}}{\Omega} & -\frac{s_y\tau_{zx}}{\Omega} & -\frac{s_z\tau_{zx}}{\Omega} & -\frac{\tau_{xy}\tau_{zx}}{\Omega} & -\frac{\tau_{yz}\tau_{zx}}{\Omega} & \frac{1}{2}-\frac{\tau_{zx}^2}{\Omega} & \end{bmatrix} \tag{11}$$

where

$$\Omega = \frac{2}{3}\bar{\sigma}^2\left(1+\frac{H}{3G}\right) \tag{12}$$

and E and G are Young's and shear moduli, respectively, ν is Poisson's ratio, $\bar{\sigma}$ the effective stress and H the plastic modulus.

To preserve the quadratic rate for asymptotic convergence, the integration algorithm must be consistent with the tangent operator. However, this becomes true only when the *path-dependent strategy* for strain increment is used in the above operator. This indicates that the constitutive equations should be integrated based on the corrective strain increment at the iteration step i when the non-converged results at step $i-1$ is used as the initial conditions.[16] Unfortunately, this strategy is not realistic because of some obvious disadvantages, such as the poor estimation of plastic flow over the iterations and false indication of elastic unloading.

3.2.2. Consistent operator. The consistent operator can overcome the above difficulties. By following the approach (1-c), and making use of elastic predictor-radial corrector and equation (10), an elastic–plastic consistent tangent operator can be derived

$$\mathbf{C}_{ep} = \begin{bmatrix} \Lambda - Ns_x^2 & & & & & \text{Sym.} \\ \Gamma - Ns_y s_x & \Lambda - Ns_y^2 & & & & \\ \Gamma - Ns_z s_x & \Gamma - Ns_z s_y & \Lambda - Ns_z^2 & & & \\ -N\tau_{xy}s_x & -N\tau_{xy}s_y & -N\tau_{xy}s_z & G\bar{\beta} - N\tau_{xy}^2 & & \\ -N\tau_{yz}s_x & N\tau_{yz}s_y & -N\tau_{yz}s_z & -N\tau_{yz}\tau_{xy} & G\bar{\beta} - N\tau_{yz}^2 & \\ -N\tau_{zx}s_x & -N\tau_{zx}s_y & -N\tau_{zx}s_z & -N\tau_{zx}\tau_{xy} & -N\tau_{zx}\tau_{yz} & G\bar{\beta} - N\tau_{zx}^2 \end{bmatrix} \tag{13}$$

where Λ, Γ and N are defined by

$$\Lambda = K + \tfrac{4}{3} G\bar{\beta} \tag{14}$$

$$\Gamma = K - \tfrac{2}{3} G\bar{\beta} \tag{15}$$

$$N = \frac{3G\bar{\gamma}}{\bar{\sigma}^2} \tag{16}$$

where K is the bulk modulus of the material and factors $\bar{\beta}$ and $\bar{\gamma}$ are given by

$$\bar{\beta} = \left(\frac{\mathbf{s}^i_{n+1} \cdot \mathbf{s}^i_{n+1}}{\mathbf{s}^i_{\mathrm{T}} \cdot \mathbf{s}^i_{\mathrm{T}}} \right)^{1/2} \tag{17}$$

$$\bar{\gamma} = \left(\frac{1}{1 + (H/3G)} \right) + \bar{\beta} - 1 \tag{18}$$

In equation (17), $\mathbf{s}_{\mathrm{T}}$ is the trial deviatoric stress based on an assumption of elastic behaviour. The above consistent tangent operator can easily be applied to the *path-independent updating strategy*. In this strategy, the integration of constitutive equations during each iteration are always based on the total strain increment of the load step, and the initial conditions are the converged results of the last load step.[16] It is extremely important for plasticity analysis.

It is interesting to note that if very small load steps are used, $\bar{\beta} \to 1$, and the continuum and consistent algorithms will bring about identical solutions. If the load steps are large, however, $\bar{\beta}$ will be significantly less than a unit and the two algorithms will go far away from each other.

4. THE CONSISTENT DXDR ALGORITHM

4.1. The algorithm

According to the discussion above, a complete consistent DXDR algorithm is proposed as follows:

(a) $J = 0$, specify $N_{\max}$, e_{R}, e_k, and $J_{\max}$, where J is the number of load steps,
(b) apply a new external load increment, $J = J + 1$,
(c) $\dot{\mathbf{X}}^0 = 0$, $n = 0$; specify $\mathbf{X}^0$,
(d) $\zeta^0_i = 0$ $(i = 1, \ldots, N_{\mathrm{total}})$; exert boundary conditions,
(e) determine $\tilde{\mathbf{X}}^0$ and iterate if necessary,
(f) form $\mathbf{M}$,
(g) compute $\mathrm{d}\varepsilon^n$,
(h) if the node was elastic in the last load step, continue, otherwise turn to (*j*),

(i) if the node is still elastic (this must be true when $n = 0$), $\mathrm{d}\sigma^n = \mathrm{d}\sigma^n_{\mathrm{e}}$, and turn to (*k*), if it becomes plastic, $\mathrm{d}\sigma^n = (1 - \mathbf{R}^n)\mathrm{d}\sigma^n_{\mathrm{e}} + \mathbf{R}^n \mathbf{C}^n_{\mathrm{ep}} \mathrm{d}\varepsilon^n$ and turn to (*k*), where $\mathbf{R}^n = (\bar{\sigma}^n_{\mathrm{e}} - \mathbf{Y}^n)/(\bar{\sigma}^n_{\mathrm{e}} - \bar{\sigma}^n)$ is the proportional factor; if necessary, subincremental steps could be used in calculating the $\mathrm{d}\sigma^n$,

(j) if the node is still plastic (this must be true when $n = 0$), $\mathbf{d}\boldsymbol{\sigma}^n = \mathbf{C}^n_{\mathrm{ep}}\, \mathbf{d}\boldsymbol{\varepsilon}^n$ (use subincremental steps if necessary), if it becomes elastic, $\mathbf{d}\boldsymbol{\sigma}^n = \mathbf{d}\boldsymbol{\sigma}^n_{\mathrm{e}}$,

(k) temporarily update the stresses ($\boldsymbol{\sigma}^{n+1} = \boldsymbol{\sigma}^n + \mathbf{d}\boldsymbol{\sigma}^n$) and relevant variables,

(l) calculate disequilibrium force $\mathbf{R}^n$,
(m) if $|R_i^{Ln}| \leqslant e_R$ ($L = u, v, w$), turn to (t); otherwise continue,
(n) calculate ζ_i^n,
(o) obtain $\dot{\mathbf{X}}^{n+1/2}$,
(p) if $\sum_{L=u}^{w} \sum_{i=1}^{N} (\dot{x}_i^{Ln+1/2})^2 \leqslant e_k$, turn to (t); otherwise continue,
(q) calculate $\mathbf{X}^{n+1}$,
(r) apply boundary conditions,
(s) $n = n + 1$; if $n > N_{max}$, stop; otherwise return to step (f),
(t) update all corresponding variables,
(u) if $J > J_{max}$, stop; otherwise return to (b).

4.2. *Applicability*

The algorithm is developed for solving quasi-static path-dependent or path-independent problems, such as those subjected to elastic or elastic–plastic deformation, proportional or disproportional loading, and those with or without bifurcations. However, this algorithm is not suitable for studying time-dependent problems because DXDR method involves fictitious time as a variable.

The iteration stability of the algorithm is guaranteed by the instant calculation of the mass matrix $\mathbf{M}$ inside the iteration loop,[1,4,19–21] which is evaluated by using the well-known Gerschgörin theorem.[22] A proper selection of the instant node damping ζ_i^n affects greatly the convergence rate in reaching the static state in each incremental load step. Equation (5) has been proved to be a good selection.[1] Most importantly, the uniqueness of the equilibrium state obtain by a DR-type algorithm has been proved mathematically and found to be iteration-path independent.[23] In other words, the final static solution is not affected by the variation of instant $\mathbf{M}$ and ζ_i^n during iteration. Therefore, the equilibrium solution obtained by the above proposed algorithm is credible.

5. NUMERICAL EXAMPLES

Numerical results of four typical problems are presented below to show the accuracy, stability and convergence rate of the proposed consistent DXDR method. The first and second examples are elastic–plastic bending of rectangular and circular plates. The other two, an annular plate subjected to a uniform tension on its outer edge and a rectangular notched plate under an axial tension, are plane stress problems with different orders of stress concentration. The simple J_2 flow theory was used throughout the analysis. Materials were assumed to be elastic-prefectly plastic, and $E = 21\,000\ \text{kg/mm}^2$, $\nu = 0{\cdot}3$, and $Y = 20\ \text{kg/mm}^2$ were used. To compare the relative efficiency of the consistent DXDR method with ADINA code, a well-known finite element software for engineering analysis, [example 4] was calculated using a Sun Sparc Station 1. All the other calculations were carried out on a PC DIRECT 486, DX2-66.

Example 1. *The elastic–plastic bending of a simply supported square plate subjected to a uniform pressure.* The side length of the plate, a, is 120 mm and its thickness, h, is 2 mm. The incremental form of equilibrium equations can be written as

$$\frac{\partial^2 \delta M_x}{\partial x^2} + \frac{\partial^2 \delta M_y}{\partial y^2} - 2\frac{\partial^2 \delta M_{xy}}{\partial x \partial y} + \delta q = 0 \tag{19}$$

where

$$(\delta M_x, \delta M_y, \delta M_{xy}) = \int_{-h/2}^{h/2} (z\delta\sigma_x, z\delta\sigma_y, z\delta\tau_{xy})\mathrm{d}z \tag{20}$$

The relations between strains and displacements are

$$\delta\varepsilon_x = z\delta\kappa_x, \quad \delta\varepsilon_y = z\delta\kappa_y, \quad \delta\gamma_{xy} = 2z\delta\kappa_{xy} \tag{21}$$

where

$$\delta k_x = -\frac{\partial^2\delta w}{\partial x^2}, \quad \delta k_y = -\frac{\partial^2\delta w}{\partial y^2}, \quad \delta k_{xy} = \frac{\partial^2\delta w}{\partial x\partial y} \tag{22}$$

The results obtained for different algorithms are compared with Dinis' solution[17] in Figure 1.

Example 2. *An elastic–plastic clamped circular plate in large deflection.* The plate is of radius $R = 120$ mm and thickness $h = 4$ mm. The incremental equilibrium equations are therefore

$$\begin{aligned} &\frac{\partial^2\delta M_r}{\partial r^2} + \frac{1}{r}\left(2\frac{\partial\delta M_r}{\partial r} - \frac{\partial\delta M_\theta}{\partial r}\right) + (N_r + \delta N_r)\frac{\partial^2\delta w}{\partial r^2} \\ &\quad + \delta N_r\frac{\partial^2 w}{\partial r^2} + \frac{1}{r}\left[(N_\theta + \delta N_\theta)\frac{\partial\delta w}{\partial r} + \delta N_\theta\frac{\partial w}{\partial r}\right] + \delta q = 0 \\ &\frac{\partial\delta N_r}{\partial r} + \frac{1}{r}(\delta N_r - \delta N_\theta) = 0 \end{aligned} \tag{23}$$

where

$$(N_r, N_\theta, M_r, M_\theta) = \int_{-h/2}^{h/2} (\sigma_r, \sigma_\theta, z\sigma_r, z\sigma_\theta)\mathrm{d}z \tag{24}$$

are the membrane forces and the bending moments in the radial and circumferential directions, respectively. The geometrical relations between strains and displacements are

$$\delta\varepsilon_r = \delta\varepsilon_r^0 + z\delta\kappa_r, \quad \delta\varepsilon_\theta = \delta\varepsilon_\theta^0 + z\delta\kappa_\theta \tag{25}$$

where

$$\begin{aligned} &\delta\varepsilon_r^0 = \frac{\partial\delta u}{\partial r} + \frac{\partial w}{\partial r}\frac{\partial\delta w}{\partial r} + \frac{1}{2}\left(\frac{\partial\delta w}{\partial r}\right)^2 \\ &\delta\varepsilon_\theta^0 = \frac{\delta u}{r}, \quad \delta k_r = -\frac{\partial^2\delta w}{\partial r^2}, \quad \delta k_\theta = -\frac{1}{r}\frac{\partial\delta w}{\partial r} \end{aligned} \tag{26}$$

The calculation results obtained from two algorithms are compared with Crose's results[18] in Figure 2.

Example 3. *An annular plate with a uniform tension on its outer edge.* The inner and outer radii, R_i and R_o, are respectively 30 and 300 mm and the plate thickness is 2 mm. In this case, the only equilibrium equation is

$$\frac{\partial\delta\sigma_r}{\partial r} + \frac{1}{r}(\delta\sigma_r - \delta\sigma_\theta) = 0 \tag{27}$$

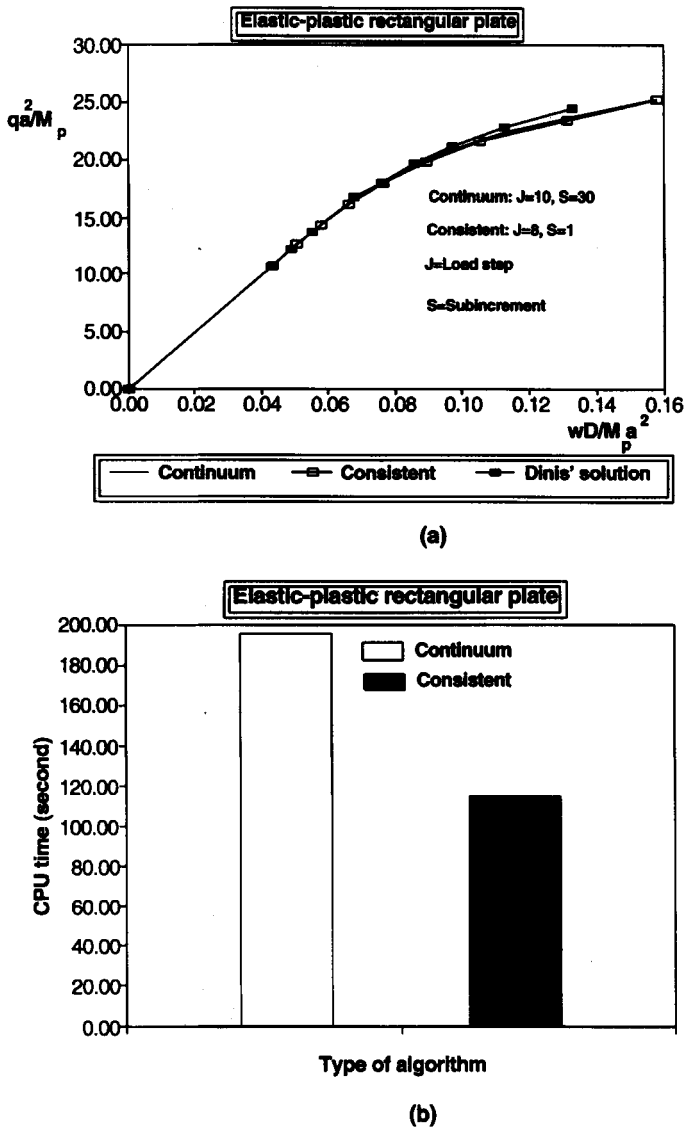

Figure 1. Elastic–plastic load–deflection curves and comparison of CPU times for square plate: (a) central load–deflection curve, (b) comparison of CPU time

and the geometrical relations are

$$\delta\varepsilon_r = \frac{\partial \delta u}{\partial r}, \quad \delta\varepsilon_\theta = \frac{\delta u}{r} \tag{28}$$

A comparison between the two integration algorithms is shown in Figure 3.

Example 4. An elastic–plastic notched rectangular plate under an in-plane tension (Figure 4(a)). The length a, width b, and thickness h of the plate are 200, 160 and 2 mm, respectively. The

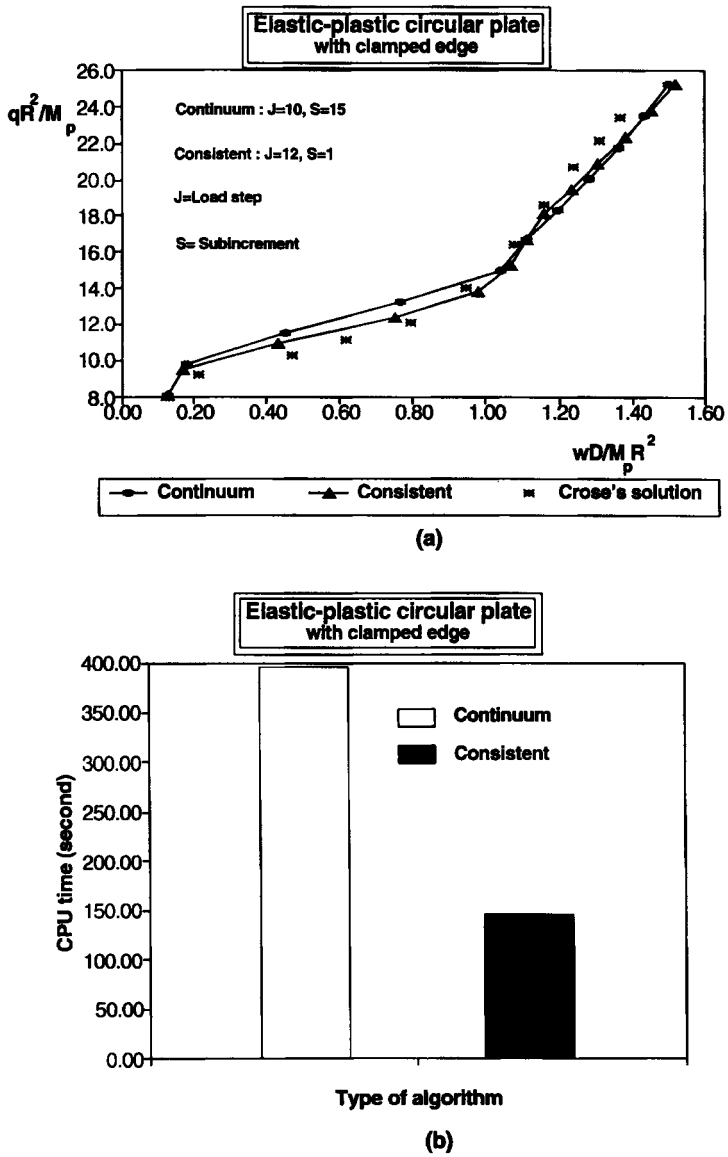

Figure 2. Elastic–plastic load–deflection curves and comparison of CPU times for circular plate: (a) central load–deflection curve, (b) comparison of CPU time

equilibrium equations for this problem are

$$\frac{\partial \delta N_x}{\partial x} + \frac{\partial \delta N_{xy}}{\partial y} = 0, \quad \frac{\partial \delta N_y}{\partial y} + \frac{\partial \delta N_{xy}}{\partial x} = 0 \tag{29}$$

and the relations between strains and displacements are

$$\delta \varepsilon_x = \frac{\partial \delta u}{\partial x}, \quad \partial \varepsilon_y = \frac{\partial \delta v}{\partial y} \tag{30}$$

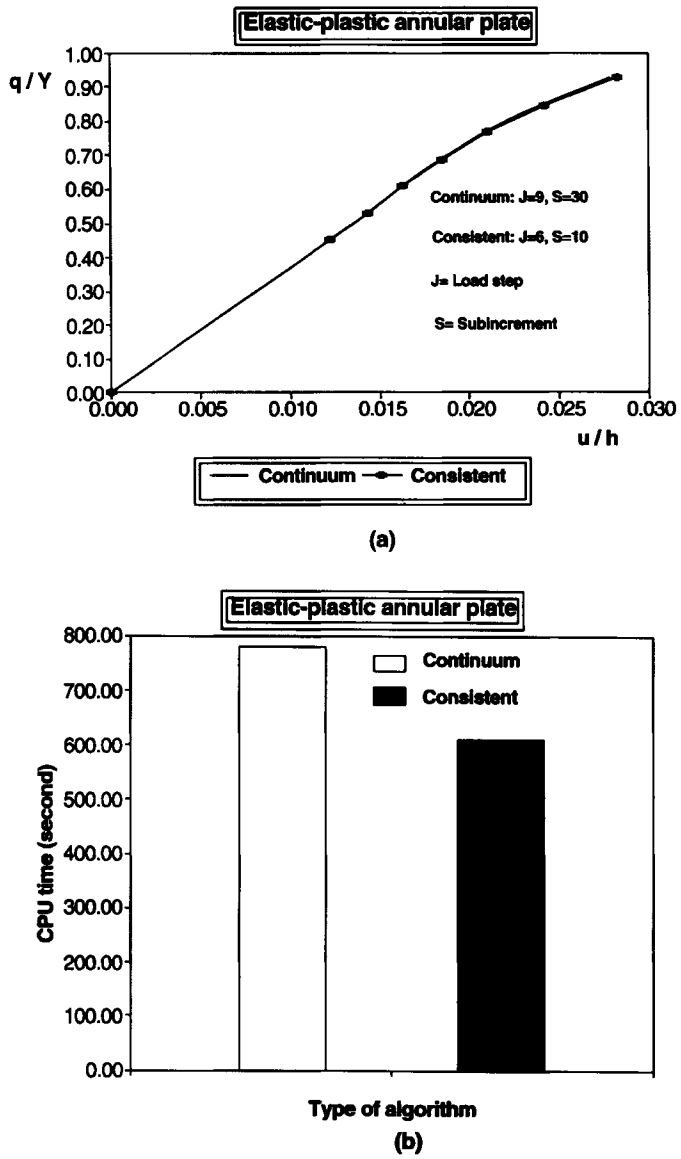

Figure 3. Elastic–plastic load–deflection curves and comparison of CPU times for annular plate: (a) load–deflection curve at $r = R_i$, (b) comparison of CPU time

The results obtained from both the continuum and consistent algorithms are compared with ADINA calculations in Figures 4(b), (c).

6. DISCUSSION

To demonstrate the merits of the proposed consistent DXDR method in analysing elastic–plastic problems, comparisons have been made in the following manners: (a) the CPU time required under the same accuracy criterion, which indicates the efficiency of the method, (b) the

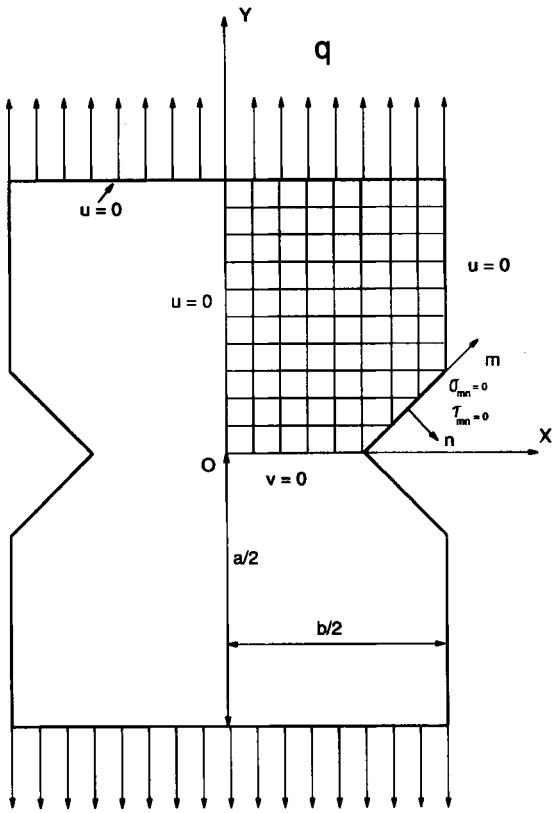

(a)

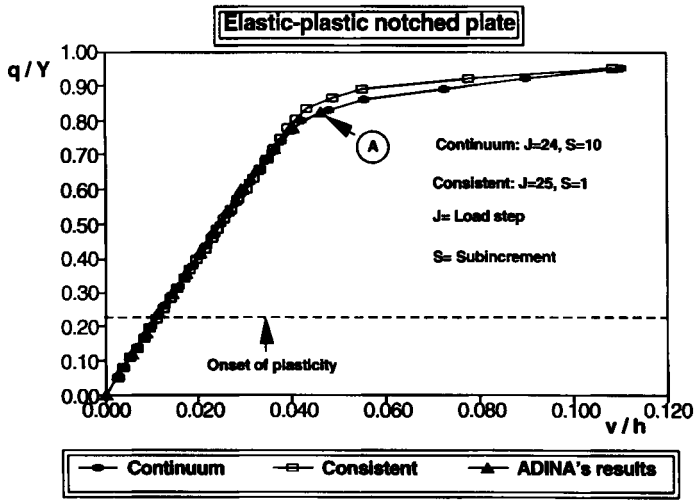

(b)

Figure 4. (a, b)

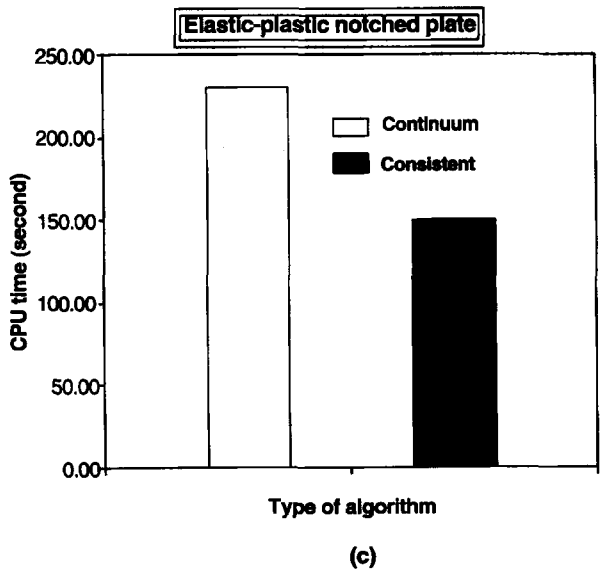

Figure 4. Elastic–plastic load–deflection curves and comparison of CPU times for notched plate: (a) mesh and boundary conditions, (b) load–deflection curve at $(X, Y) = (0, a/2)$, (c) comparison of CPU time

convergence history of the disequilibrium force and kinetic energy, which shows the convergence rate of the algorithm, (c) the stability of the new algorithm and (d) the compatibility of the DXDR method with the consistent elastic–plastic operator.

Figures 1(a), (b), 2(a), (b) 3(a), (b) and 4(b), (c) clearly show that the present consistent DXDR method is extremely efficient in comparison with the commonly used continuum algorithm. A significant reduction of CPU time of 25–60 per cent can always be obtained in all the examples (the accuracy of the results was kept the same). This method is also more efficient than the relevant approach used by ADINA. In the calculation of the notched plate, the consistent DXDR method saved up to 40 per cent of CPU time compared with the ADINA code under the same accuracy criterion, see Figures 4(b) and 6.

There is a distinct effect of the consistent algorithm on the convergence rate of the DXDR method. This could be observed through the norm variations of the kinetic energy and residual force during the DXDR iteration. Figure 5 shows the convergence history of the norms in calculating the circular and notched plates when the total incremental steps have been the same for both continuum and consistent algorithms. Obviously, the consistent algorithm provides higher convergence rate. Generally, there are three key factors which influence the convergence of the DR-type methods:[1] the initial vector $\mathbf{X}^0$, the fictitious mass matrix $\mathbf{M}$, and the critical node damping factor ζ. In the present calculations, the initial vectors for both methods were the same. Thus $\mathbf{X}^0$ would not have any effect on the final computation time. The instant critical node damping factor ζ, however, is basically determined by the Rayleigh quotient so that only one of the frequencies of the fictitious transient system is damped critically and the rests are in under-/over-damped states. In other words, the closer the highest and lowest frequencies, the higher the convergence rate would be. Therefore, the high convergence rate of the consistent DXDR method could be due to the alternation of the frequencies. This, in turn, improves the evaluation of the instant mass matrix $\mathbf{M}$ as well.

To show the reliable stability attainable of the new method, a comparison between the new algorithm and the ADINA code, with a same mesh, is made for the elastic–plastic tension of the

notched plate (Figure (4(a)). The 2-D solid element was used in ADINA calculation. The consistent DXDR method was always stable until the whole section of the plate became plastic. The ADINA calculation, however, failed because of numerical instability where the load q/Y went beyond 0·825 (point A in Figure 4(b)), although very small load steps had been used (240 load steps after point A). The number of load steps of the consistent DXDR method were only 25 after the onset of plasticity. It is evident from Figure 4(b) that although the slope of the load deflection curve becomes very small beyond point A, the present method was still incredibly reliable in seeking the equilibrium state of the mechanics system.

The compatibility between the two components of the new algorithm could be the origin of all the achieved merits discussed above. It means that the consistent elastic–plastic operator not only

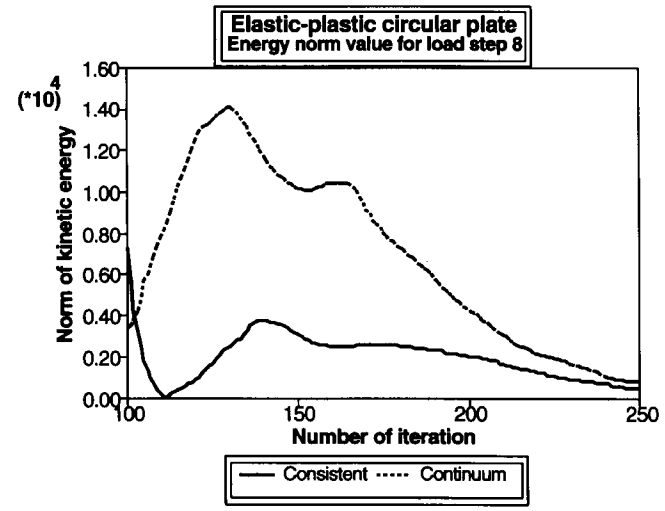

(a)

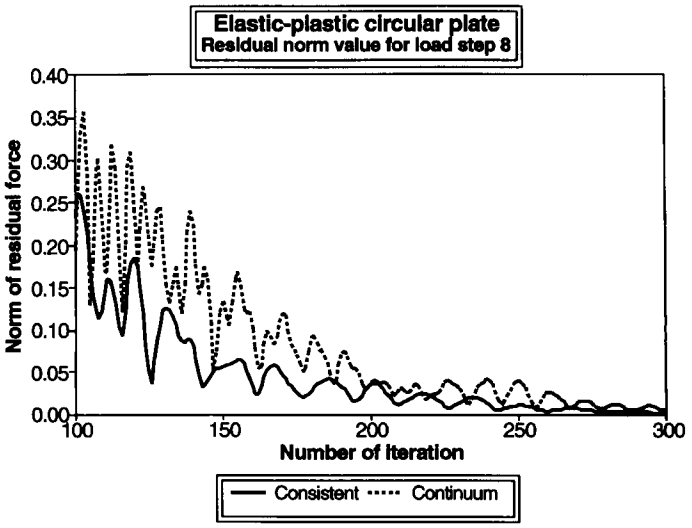

(b)

Figure 5. (a, b)

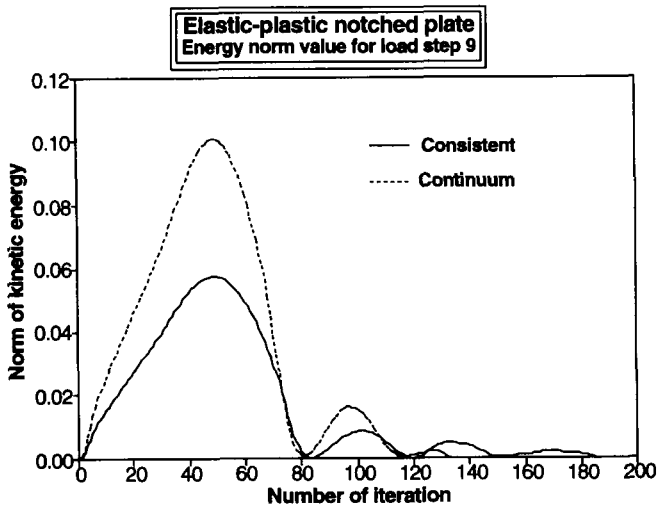

(c)

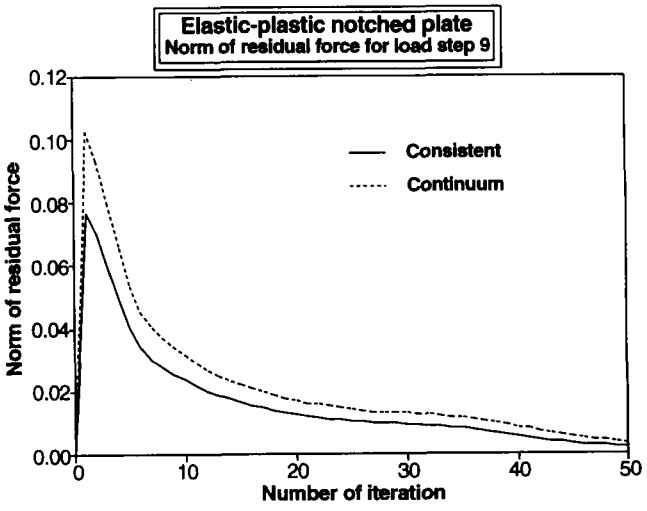

(d)

Figure 5. Convergence history of the norm of kinetic energy and residual force: (a) norm of kinetic energy of the circular plate, (b) norm of residual force of the circular plate, (c) norm of kinetic energy of the notched plate, (d) norm of residual force of the notched plate

allows much larger incremental steps through its unconditionally stable integration scheme, but also enhances the convergence rate of the DXDR method by, somehow, improving the evaluation of the instant critical node damping factor ζ and mass matrix $\mathbf{M}$.

As discussed in Section 4.2, the present consistent DXDR method is powerful for solving quasi-static elastic–plastic problems. For instance, although the loading paths in the elastic–plastic bending of the circular plate with large deflection (example 2) and the elastic–plastic tension of the notched plate (example 4) were extremely disproportional, see Figure 7, the new algorithm provided credible and accurate results.

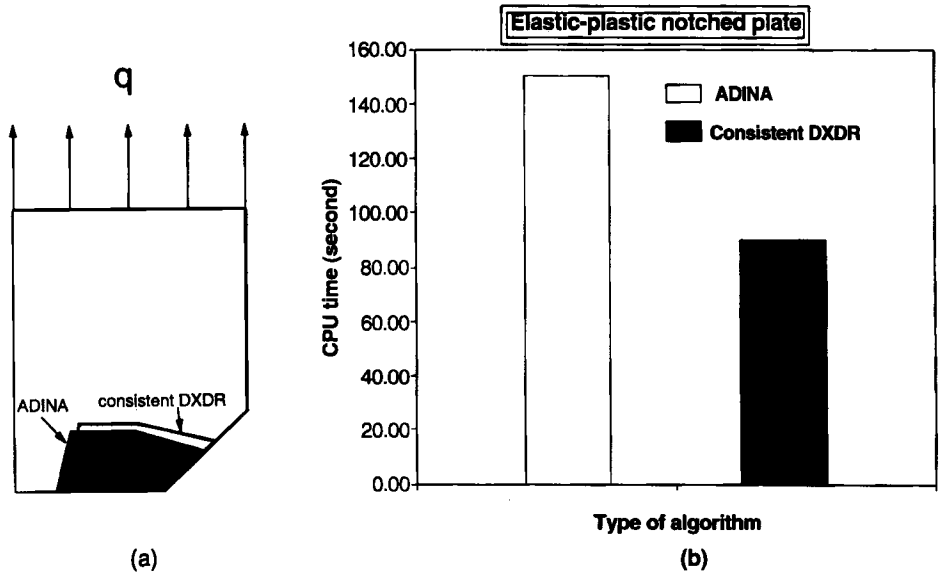

Figure 6. Comparison between the performance of the consistent DXDR method and ADINA code: (a) plastic zone ($q/Y = 0{\cdot}825$), (b) CPU time

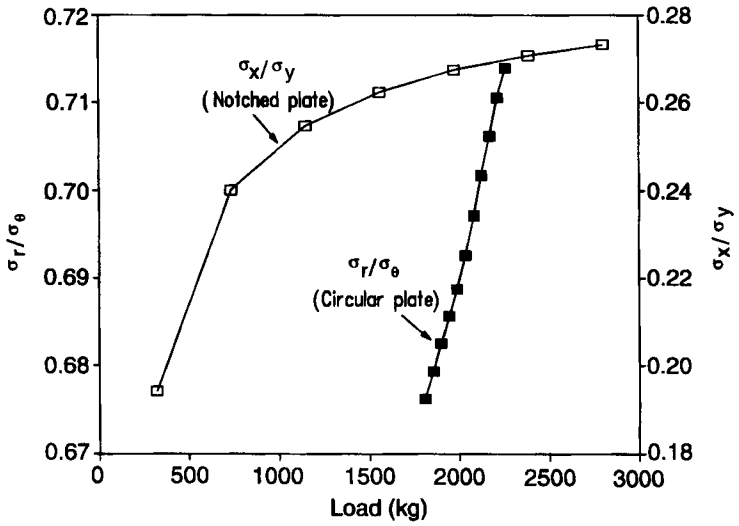

Figure 7. Variation of σ_r/σ_θ at point A and σ_x/σ_y at point B during loading in the circular and notched plates (co-ordinate of point A: $(r, z) = (60, 2)$ (mm) and that of point B: $(x, y, z) = (40, 50, 1)$ (mm))

7. CONCLUSIONS

A new promising method, the consistent DXDR method, has been proposed by combining the consistent return mapping technique with the DXDR algorithm. Compared with previous algorithms, this method allows to use much larger incremental loading steps under a given accuracy and offers very stable ability in seeking equilibrium states. The efficiency of computation

and potential of application of this method in analysing elastic–plastic problems have clearly been demonstrated through different types of engineering examples. It has been found that this new method possesses all the merits of the DXDR algorithm and the consistent return mapping technique, and offers an adequate convergence rate with reliable stability.

ACKNOWLEDGEMENT

This work is sponsored by ARC Small Grant. ADINA code was used to calculate an example for comparison.

NOTATION

- a length of a rectangular plate
- b width of a rectangular plate
- $\mathbf{C}$ diagonal damping matrix $[c_{ii}]$
- $\mathbf{C}_{ep}$ elastic–plastic stress–strain matrix
- D flexural rigidity of a plate, $Eh^3/12(1-\nu^2)$
- E Young's modulus
- $\mathbf{e}$ deviatoric strain
- e_k, e_R the convergence indexes of the energy and residual force of the dynamic system defined by equation (2)
- $\mathbf{F}$ vector of generalized external forces of a discrete system
- G shear modulus
- h thickness of a plate
- H plastic modulus
- J number of load step
- $\mathbf{K}$ stiffness matrix of the discrete system (equation (8))
- K bulk modulus
- $\mathbf{M}$ diagonal mass matrix of the discrete system $[m_{ii}^L]$
- M bending or twisting moment
- M_p fully plastic bending moment, $1/4\ Yt^2$
- N member force
- N_{total} total node number of the discrete system
- N_{max} maximum iteration number with respect to fictitious time
- $\mathbf{n}$ unit normal vector at the contact point of the yield surface
- $\mathbf{P}$ vector of internal forces of the discrete system (equation (1))
- q uniformly distributed transverse load
- $\mathbf{R}$ vector of residual forces of the discrete system
- R radius of a circular plate
- R_i inner radius of an annular plate
- R_o outer radius of an annular plate
- S number of subincrement in each load step
- $\mathbf{s}$ deviatoric stress
- u, v, w displacement components in x, y and z directions, respectively
- $\mathbf{X}$ vector of generalized solution of the discrete system
- $\dot{\mathbf{X}}, \ddot{\mathbf{X}}$ vectors of fictitious velocity and acceleration of the discrete system, respectively
- Y yield stress
- z direction normal to the mid-plane of the plate

γ shear strain
$\delta(\ldots)$ a small increment of quantity $(\ldots)$
κ curvature of the plate
ε normal strain
λ incremental parameter, defined by equation (9b)
ν Poisson's ratio
ζ critical node damping factor
σ normal stress
$\bar{\sigma}$ effective stress
τ_{ij} shear stress component
τ increment of fictitious time
ϕ von Mises yield function

Superscripts and subscripts

i node i
L indication of three perpendicular directions coincident with displacement u, v, and w, respectively
n the nth iteration step
x, y x and y directions, respectively
r, θ r and θ directions, respectively

REFERENCES

1. L. C. Zhang, M. Kadkhodayan and Y.-W. Mai, 'Development of maDR method', *Comput. Struct.*, **52**, 1–8 (1994).
2. J. C. Simo and R. L. Taylor, 'Consistent tangent operators for rate-independent elastoplasticity', *Comput. Methods Appl. Mech. Eng.*, **48**, 101–118 (1985).
3. P. Underwood, 'Dynamic relaxation', in T. Belytschkev and T. J. R. Hughes (eds.), *Computational Methods for Transient Analysis*, Elsevier, Amsterdam, 1983, p. 245.
4. L. C. Zhang and T. X. Yu, 'Modified adaptive dynamic relaxation method and its application to elastic–plastic bending and wrinkling of circular plates', *Comput. Struct.*, **33**, 609–614 (1989).
5. M. Ortiz and E. P. Popov, 'Accuracy and stability of integration algorithm for elastoplastic constitutive relations', *Int. j. numer. methods eng.*, **21**, 1561–1576 (1985).
6. J. C. Nagtegaal and J. E. de Jong, 'Some computational aspects of elastic–plastic large strain analysis', *Int. j. numer. methods eng.*, **17**, 15–41 (1981).
7. R. D. Krieg and D. B. Krieg, 'Accuracies of numerical solution methods for the elastic-perfectly plastic model', *Trans. ASME, J. Press, Vessel Tech.*, **99**, 510–515 (1977).
8. H. L. Schreyer, R. F. Kulak and J. M. Kramer, 'Accurate numerical solutions for elastic-plastic models', *Trans. ASME, J. Press, Vessel Tech.*, **101**, 226–234 (1979).
9. J. R. Rice and D. M. Tracy, 'Computational fracture mechanics', in S. J. Fenves *et al.* (eds.), *Proc. Symp. Num. Mech. Struct. Mech.*, Urbana, Illinois, 1971, Academic Press, New York, 1973, p. 585.
10. M. L. Wilkins, 'Calculation of elastic-plastic flow', in B. Alder *et al.* (eds.), *Methods of Computational Physics*, Vol. 3. Academic Press, New York, 1964.
11. A. Mendelson, *Plasticity: Theory and Application*, Macmillan, New York, 1968.
12. J. H. Argyris, J. St. Doltsinis, W. C. Knudson, L. E. Vaz and K. S. William, Numerical solution of transient nonlinear problem, *Comput. Methods Appl. Mech. Eng.*, **17/18**, 341–409 (1979).
13. M. Ortiz and J. C. Simo, 'An analysis of a new class of integration algorithms for elastoplastic constitutive relations', *Int. j. numer. methods eng.*, **23**, 353–366 (1986).
14. R. D. Krieg and S. W. Key, 'Implementation of a time dependent plasticity theory into structural computer programs', in J. A. Stricklin and K. J. Saczalski (eds.), *Constitutive Equations in Viscoplasticity: Computational and Engineering Aspects*, AMD-20, ASME, New York, 1976, p. 125.
15. P. J. Yoder and R. L. Whirley, 'On the numerical implementation of elastoplastic models', *J. Appl. Mech. ASME*, **51**, 283–288 (1984).
16. Robert H. Dodds, Jr, 'Numerical techniques for plasticity computations in finite element analysis', *Comput. Struct.*, **26**, 767–779 (1987).
17. L. M. S. Dinis, R. A. F. Martins and D. R. J. Owen, 'Material and geometrically nonlinear analysis of thin plates and arbitrary shells', in C. Taylor, E. Hinton and D. R. J. Owen (eds.), *Numerical Methods for Non-linear Problems*, Vol. 1., Pineridge Press, West Cross, Swansea, U.K., 1980, p. 425.

18. James G. Crose and Alfredo H.-S. Ang, 'Nonlinear analysis method for circular plates', *J. Eng. Mech. Div.* ASCE, **EM 4,** 979–999 (1969).
19. L. C. Zhang, T. X. Yu and R. Wang, 'Investigation of sheet metal forming by bending—Part II: Plastic wrinkling of circular sheets pressed by cylindrical punches, *Int. J. Mech. Sci.*, **31,** 301–308 (1989).
20. L. C. Zhang, T. X. Yu and R. Wang, 'Investigation of sheet metal forming by bending—Part I: Axisymmetric elastic–plastic bending of circular sheets pressed by cylindrical punches', *Int. J. Mech. Sci.*, **31,** 285–300 (1989).
21. L. C. Zhang, T. X. Yu and R. Wang, 'Investigation of sheet metal forming by bending—Part III: Applicability of deformation theory to stamping of circular sheets', *Int. J. Mech. Sci.*, **31,** 327–333 (1989).
22. W. A. Watson, T. Philipson and P. J. Oates, '*Numerical analysis*', *The Mathematics of Computing*, 2nd edn., Edward Arnold, London, 1981.
23. C. A. Felippa, 'Dynamic relaxation and quasi-Newton methods', in C. Taylor, E. Hinton, D. R. J. Owen and E. Onate (eds.), *Numerical Methods for Nonlinear Problems*, Vol. 2, Pineridge Press, Swansea, U.K., 1984, p. 27.

The author has requested enhancement of the downloaded file. All in-text references underlined in blue are linked to publications on Resea